FOURTH-ORDER ACCURATE FINITE-DIFFERENCE METHOD TO THE THREE

DIMENSIONAL COMPRESSIBLE BOUNDARY LAYER EQUATIONS

SAMIR F. RADWAN [*]

ABSTRACT

This paper presents a fourth-order accurate finite-difference method for solving the full three-dimensional compressible boundary layer equations, for both subsonic and supersonic laminar flows over configurations with aerospace interest, in particular, swept wing and ellipsoid. The governing equations are written in non-orthogonal surface oriented coordinates to allow maximum flexibility in the calculations, and then are solved in similarity type transformed coordinates for their well advantages over the physical coordinates.

The numerical scheme is an implicit finite-difference scheme with a fourth-order accuracy. It is unconditional stable, even for reversal cross-flow cases, where it is modified to satisfy the Courant-Friedrich-Levy condition. The resulting finite-difference equations form a non-linear block tridiagonal system. Newton's method is used to linearize it , and the LU-factorization method is used solve the linearized block tridiagonal system. The present method has been tested for validation. The subsonic flows over swept wing as well as a prolate spheroid are computed. Also, the case of supersonic flow, at mach number M=1.5 , past a prolate spheroid is calculated successfully. In each case, all the flow quantities such as velocity and temperature profiles, skin friction coefficients, and the boundary layer thicknesses are obtained.

[*]   Assistant Professor, Department of Engineering Mathematics and Physics, Faculty of Engineering, Alexandria University, El-Shatbey, Alexandria, EGYPT

INTRODUCTION

The numerical solution of the three-dimensional boundary layer equations is of interest in several areas in fluid dynamics. Many investigators have developed different numerical schemes to compute laminar and turbulent flowfields of different configurations in direct and inverse modes. A survey of the literature [1-7] indicates that these methods are limited to second-order accurate methods as well as to specific flow cases. Therefore, in the present study, a finite-difference method with a fourth-order accuracy will be developed to solve the full 3-D compressible boundary layer equations for aerospace configurations.

High-order accurate boundary layer solutions are required in the studies of laminar flow stability as well as in the calculations of high speed flows by the viscous/inviscid interacting procedure. Also, the high-order accurate methods can be used to obtain solutions as accurate as the second-order accurate methods, but with less grid points. For more informations about these methods see Wornom [8] . Attention, in the present study, is given to the compact finite-difference schemes. They consist of finite-difference schemes that involve two or three grid points and treat the functional and its derivative as unknowns. The two-point compact schemes have the advantage that they have fourth order accuracy even for non-uniform grids. Liniger [9] have analysed their numerical stability as schemes for the initial value problems, and Wornom [8] have used them for two-dimensional incompressible boundary layers.

The primary objective of the present work is to demonstrate the feasibility of the compact scheme with fourth-order accuracy to the solution of the 3-D compressible boundary layer equations, for flows over aerospace configurations.

FORMULATION OF THE PROBLEM

Consider a steady, compressible, laminar fluid flow of density ρ, and viscosity coefficient μ. The governing equations, based on the first-order boundary layer theory and written in surface oriented coordinated, take the following form :

(i) Continuity Equation :

$$\frac{\partial}{\partial x}(C_{11}\rho u) + \frac{\partial}{\partial y}(C_{12}\rho v) + \frac{\partial}{\partial z}(C_{13}\rho \widetilde{w}) = 0 \tag{1}$$

(ii) Momentum Equations :

$$C_{21}u\frac{\partial u}{\partial x} + C_{22}v\frac{\partial u}{\partial y} + C_{23}\widetilde{w}\frac{\partial u}{\partial z} + C_{24}u^2 + C_{25}uv + C_{26}v^2 = C_{27}\frac{\partial p}{\partial x} + C_{28}\frac{\partial p}{\partial y} + \frac{1}{\rho}\frac{\partial}{\partial z}\tau_{xz} \tag{2}$$

$$C_{31}u\frac{\partial v}{\partial x} + C_{32}v\frac{\partial v}{\partial y} + C_{33}\widetilde{w}\frac{\partial v}{\partial z} + C_{34}u^2 + C_{35}uv + C_{36}v^2 = C_{37}\frac{\partial p}{\partial x} + C_{38}\frac{\partial p}{\partial y} + \frac{1}{\rho}\frac{\partial}{\partial z}\tau_{yz} \tag{3}$$

(iii) Energy Equation :

$$C_{41}u\frac{\partial H}{\partial x} + C_{42}v\frac{\partial H}{\partial y} + C_{43}\widetilde{w}\frac{\partial H}{\partial z} = \frac{1}{\rho}\frac{\partial}{\partial z}\left[\mu\frac{\partial(\frac{1}{2}q^2)}{\partial z} - Q'\right] \tag{4}$$

where

$$\tau_{xz} = \mu\frac{\partial u}{\partial z} \quad , \qquad \tau_{yz} = \mu\frac{\partial v}{\partial z} \tag{5a}$$

$$H = c_p T + .5\, q^2 \quad , \qquad q^2 = u^2 + v^2 + \frac{2a_{12}}{h_1 h_2} uv \tag{5b}$$

$$-Q = \frac{\mu}{Pr}\left(\frac{\partial H}{\partial z} - \widetilde{w}H\right) - \frac{\mu}{Pr}\frac{\partial}{\partial z}(.5\, q^2) \tag{5c}$$

The velocity components $u, v, \widetilde{w}$, are in x,y, and z coordinate-directions respectively. The pressure and the temperature of the fluid flow are denated by p, and T . Also, Pr is the Prandtl number, and a_{ij} is the metric tensor of the

body surface. The free-stream velocity U_∞, and a reference length L, are used to non-dimensionalized the governing equations. The viscosity is assumed to vary according to Sutherland's law, and only ideal gases are considered. The coefficients C_{ij} are known functions of the metric tensor components (h_1, h_2, a_{12}) and their partial derivatives with respect to x and y.

Boundary Conditions

i- The no-slip condition is specified at the body surface

$$u = v = 0 \quad , \quad w = f(x,y) \qquad \text{at} \quad z = 0 \qquad (6a)$$

$$T = T_w(x,y) \quad , \quad \text{or} \quad \frac{\partial H}{\partial z} = g(x,y) \quad \text{at} \quad z = 0 \qquad (6b)$$

where, $f(x,y)$ is the surface injection or suction velocity. For energy equation, the wall temperature or wall heat flux can be specified.

ii- The inviscid flow solution is imposed at the edge of the boundary layer.

$$u = u_e(x,y) \quad , \quad v = v_e(x,y) \quad , \quad H = H_e(x,y) \qquad \text{at} \quad z \to \infty \qquad (6c)$$

The governing equations (1-6) form a system of coupled non-linear partial differential equations. They are a mixed type of parabolic and hyperbolic PDEs that can be solved as initial value problem.

Transformation of the Equations

The governing equations (1-6) are transformed by using a similarity type transformation that removes the singularity at the leading edge, and eliminates large streamwise variation in the solution. It have the form :

$$\frac{\partial}{\partial x} = \frac{\partial}{\partial \xi} + \frac{\partial}{\partial \zeta} \frac{\partial \zeta}{\partial x} \qquad (7a)$$

$$\frac{\partial}{\partial y} = \frac{\partial}{\partial \eta} + \frac{\partial}{\partial \zeta} \frac{\partial \zeta}{\partial y} \qquad (7b)$$

$$\frac{\partial}{\partial z} = \frac{\partial}{\partial \zeta} \frac{\partial \zeta}{\partial z} \qquad (7c)$$

such that

$$\zeta = \left[\frac{u_e}{(\rho\mu)_e s_1} \right]^{1/2} \int_0^z \rho \, dz \qquad ; \qquad s_1 = \int_o^x h_1(x,y) dx \qquad (7d)$$

$$F = u/u_e \quad ; \quad G = v/v_r \quad ; \quad E = H/H_e \qquad (7e)$$

$$v_r = u_e \text{ or } v_e \quad ; \quad C_r = v_r/u_e \qquad (7f)$$

Apply the above transformation to the continuity, a transformed normal velocity W can be obtained as follows :

$$W = . \frac{s_1}{u_e} \frac{\partial \zeta}{\partial z} w + s_1 C_{11} \frac{\partial \zeta}{\partial x} F + s_1 C_{22} C_r \frac{\partial \zeta}{\partial y} G . \qquad (8)$$

and the convective operator $\mathbb{D}$ can be written as :

$$\mathbb{D} = C_{i1} u \frac{\partial}{\partial x} + C_{i2} v \frac{\partial}{\partial y} + C_{i3} w \frac{\partial}{\partial z}$$

$$= C_{i1} u_e F \frac{\partial}{\partial \xi} + C_{i2} v_r G \frac{\partial}{\partial \eta} + \frac{u_e}{s_1} W \frac{\partial}{\partial \zeta} \qquad (9)$$

Using the transformation equations (7) and equations (8-9), the governing equations can be written in the transformed coordinates, as follows :

$$\frac{\partial W}{\partial \zeta} = A_1 \frac{\partial F}{\partial \xi} + A_2 F + A_3 \frac{\partial G}{\partial \eta} + A_4 G \qquad (10a)$$

$$\frac{\partial}{\partial \zeta} (\ell \frac{\partial F}{\partial \zeta} - WF) = B_1 \frac{\partial F^2}{\partial \xi} + B_2 \frac{\partial FG}{\partial \eta} + B_3 F^2 + B_4 FG + B_5 G^2 + B_6 \Theta_1 \tag{10b}$$

$$\frac{\partial}{\partial \zeta} (\ell \frac{\partial G}{\partial \zeta} - WG) = C_1 \frac{\partial FG}{\partial \xi} + C_2 \frac{\partial G^2}{\partial \eta} + C_3 F^2 + C_4 FG + C_5 G^2 + C_6 \Theta_2 \tag{10c}$$

$$\frac{\partial}{\partial \zeta} (\frac{\ell}{Pr} \frac{\partial E}{\partial \zeta} - WE) = D_1 \frac{\partial FE}{\partial \xi} + D_2 \frac{\partial GE}{\partial \eta} + D_3 FE + D_4 GE + D_5 \tag{10d}$$

$$\ell = \rho\mu/(\rho\mu)_e \quad , \quad \Theta_1 = \rho_e/\rho \tag{10e}$$

The coefficients A_i, B_i, C_i, and D_i are functions of the metric tensor, the inviscid velocity and their partial derivatives with respect to ξ, η, and ζ.

THE NUMERICAL MODEL

The present numerical method is an implicit compact finite-differences with a fourth-order accuracy in the direction normal to the wall and a second-order accuracy in the convective directions. The convective derivatives are discretized by using a three-point backward scheme as follows :

$$\frac{\partial}{\partial \xi} Q_{ij}^{k-\frac{1}{2}} = (a_1 Q_i + a_2 Q_{i-1} + a_3 Q_{i-2})_j^{k-\frac{1}{2}} + O(\Delta^2) \tag{11a}$$

$$\frac{\partial}{\partial \eta} Q_{ij}^{k-\frac{1}{2}} = (b_1 Q_j + b_2 Q_{j-1} + b_3 Q_{j-2})_i^{k-\frac{1}{2}} + O(\Delta^2) \tag{11b}$$

and the ζ derivative is discretized by using a two-point compact scheme. It takes the following form :

$$Q^k - Q^{k-1} - \Delta\zeta(c_1 \acute{Q}^k + c_2 \acute{Q}^{k-1}) - \Delta\zeta^2(c_3 \acute{\acute{Q}}^k + c_4 \acute{\acute{Q}}^{k-1}) = O(\Delta^5) \tag{11c}$$

$$\acute{Q} = \partial Q/\partial \zeta \quad , \quad c_1 = c_2 = 1/2 \quad , \quad c_3 = c_4 = -0.083 \tag{11d}$$

Krause [10] have made Von Neumann stability analysis to implicit schemes for the 3-D boundary layer equations, and have concluded that the zone of dependence principle should be satisfied in order to have stable numerical solution. In other words, the domain of dependence of the numerical scheme should include the domain of dependence of the boundary layer equations at any point in the (x,y) plane, it has the form :

$$\frac{vh_1}{uh_2} < \frac{\Delta y}{\Delta x} \tag{12}$$

The present numerical model always satisfies this principle, execpt for the case of reversed cross-flow. In this case, the zig-zag scheme is used instead of the backward scheme (11b) as the velocity component v changes sign :

$$\frac{\partial}{\partial \eta} Q_{ij}^{k-\frac{1}{2}} = (d_1 Q_{j-1} + d_2 Q_j)_i^{k-\frac{1}{2}} + (d_3 Q_j + d_4 Q_{j+1})_{i-1}^{k-\frac{1}{2}} + O(\Delta^2) \tag{13}$$

where, a_i, b_i, and d_i are simple functions of the grid step sizes in ξ and η. The resulting numerical method is always stable, and its computational molecule is shown in Figure 1.

Solution Procedure

The following procedure is for the momemtum equations (10b,c). A functional Ψ is defined such that :

$$\vec{\Psi} = \begin{bmatrix} \ell H - WF \\ \ell T - WG \\ F \\ G \end{bmatrix} \quad , \quad H = F' \quad , \quad T = G' \quad , \quad S = E' \tag{14}$$

The first and second derivatives of $\vec{\Psi}$ with respect to ζ ($\vec{\Psi}'$, $\vec{\Psi}''$) are obtained from equations (11). They involve the solution variables (F,G,H,T) and their partial derivatives with respect to ξ and η . Having substituting the vectors $\vec{\Psi}$, $\vec{\Psi}'$, $\vec{\Psi}''$ in to the compact scheme equation (11c,d), and apply the present scheme equations (11a,b), we have four nonlinear coupled finite-difference equations in the vector $U_1 = (F,G,H,T)^T$. They form a block tridiagonal system. They are linearized by using Newton's method and are solved iteratively. Inherent to Newton's method is a quadratic rate of convergence and the ability to force the solution to within a desired accuracy. The linearized system of equations form a block tridiagonal matrix of order n, as follows :

$$\begin{bmatrix} b_1 & c_1 & & & \bigcirc \\ \vdots & & & & \\ a_k & b_k & c_k & & \\ & & & c_{n-1} \\ \bigcirc & & a_n & b_n \end{bmatrix} \begin{bmatrix} \vec{\delta}_1 \\ \vdots \\ \vec{\delta}_k \\ \vdots \\ \vec{\delta}_n \end{bmatrix} \begin{bmatrix} \vec{r}_1 \\ \vdots \\ \vec{r}_k \\ \vdots \\ \vec{r}_n \end{bmatrix} \quad , \quad k=1,\ldots n \tag{15}$$

or
$$A \delta = r \tag{16}$$

where, a_k, b_k, and c_k are block matrices of order 4 at the k-level in the ζ-direction. $\vec{\delta}_k$, and $\vec{r}_k$ are the unknown vector and the right hand side vector of order 4. The vector $\vec{\delta}_k$ is equal to (F, G, H, T) and is equal to the change in the solution vector between successive iterations. The number of the grid points in the direction is n. In the same way, the energy equation is solved. However, this time , a 2X2 block tridiagonal system in the vector (E, S)^T is obtained. The numerical solution for the above block-tridiagonal systems are obtained by iteration. In each iteration, LU-factorization method is used to solve the block tridiagonal systems, as follows :

Let
$$A = L U \tag{17}$$

$$L = \begin{bmatrix} \Delta_1 & & \bigcirc \\ a_2 & & \\ & & \\ & a_n & \Delta_n \end{bmatrix} \quad , \quad U = \begin{bmatrix} I & \Gamma_1 & \\ & & \Gamma_{n-1} \\ \bigcirc & & I \end{bmatrix} \tag{18}$$

such that
$$\Delta_1 = b_1 \quad , \quad \Gamma_1 = \Delta_1^{-1} c_1 \tag{19a}$$
$$\Delta_i = b_i - a_i \Gamma_{i-1} \tag{19b}$$
$$\Gamma_i = \Delta_i^{-1} c_i \quad , \quad i=2,\ldots\ldots n \tag{19c}$$

where, Δ_k, Γ_k are square matrices of order 4 for the momentum equations. Then the block tri-diagonal system (16) becomes equivalent to the following two systems :

$$L w = r \quad , \quad U \delta = w \tag{20}$$

such that the vector $\vec{w}_k$ is a carrying vector of order 4. The final solution of the block tri-diagonal system (15) is as follows (reference [11]) :

$$\vec{w}_1 = \Delta_1^{-1} \vec{r}_1 \tag{21a}$$

$$\vec{w}_i = \Delta_i^{-1} (\vec{r}_i - b_i \vec{w}_{i-1}) \quad , \quad i=2,\ldots\ldots n \tag{21b}$$

and the backward substitution :

$$\vec{\delta}_n = \vec{w}_n \tag{22a}$$

$$\vec{\delta}_i = \vec{w}_i - \Gamma_i \vec{\delta}_{i+1} \quad , \quad i=n-1,\ldots\ldots 1 \tag{22b}$$

COMPUTED RESULTS AND DISCUSSIONS

The cases considered in the present study are limited to laminar flow. The first case is the problem of incompressible flow past a flat plate with attached cylinder. The inviscid velocity is given by Cebeci.[12] as follows:

$$u_e/U_\infty = 1 + \frac{y^2 - (x-x_0)^2}{\left[(x-x_0)^2 + y^2 \right]^2 / a^2} \tag{23a}$$

$$v_e/U_\infty = - \frac{2y(x-x_0)}{\left[(x-x_0)^2 + y^2 \right]^2 / a^2} \tag{23b}$$

The calculations are made for the case of $U_\infty = 30.5$ m/s , $a = 6.1$ cm , $x_0 = 45.7$ cm , $\Delta x = 1.22$ cm , and $\Delta y = 0.61$ cm, as shown in Figure 2. The obtained results are in good agreement with the previous results obtained by Cebeci [12] (Keller-box scheme) and by Fillo [13] (Crank-Nicolson scheme). Moreover, the present method, with only 12 grid points across the boundary layer, has the same accuracy as the second-order accurate methods with 50 grid points, as shown in Figure 2. for the cross-wise velocity profile at x=19.52 cm and y= 3.05 cm.

Having testing the numerical method for simple 3-D flow case, the compressible laminar flows over configurations with aerospace interest, like a prolate spheroid of axis ratio 4:1 and three degrees incidence, are computed for different mach numbers. The surface body coordinates are shown in Figure 3. The coordinate, ξ , is measured along the body axis, and the coordinate, η , is the arc length in the cross-wise direction. The incompressible flow case is computed first for sake of validating the present method. The obtained results reproduce efficiently all the features of the incompressible flow-field including the region of reversal cross-flow that previously obtained by Cebeci [4] , Wang [3] , and the present author [5,7] , as shown in Figure 3, for the cross-wise velocity profiles at location $\xi = 1.52$, ($0 \leqslant \xi \leqslant 2.0$). Then, the cases of M=0.3 and M=1.5 are computed. The inviscid flow is assumed to be irrotational and adiabatic with no heat transfer at the wall surface. Therefore, the potential flow theory is used to obtained the inviscid flow solution. The calculated results for the subsonic flow case are shown in Figures 4 and 5, for the cross-wise skin friction coefficient c_{f_y} and the wall flow directions. The present numerical method produces the features of the flowfield with a few grid points across the boundary layer, as low as 12 points. For the super-

sonic flow case, M=1.5, the method of solution marches successfully throughout the flow field including the region of large reversal cross-flows. Figure 6 shows the cross-wise velocity profiles at location ξ = 1.5, where the reversed cross-wise flows are predicted. The effect of compressiblity is shown in Figures 7 and 8, for the temperature profiles at ξ = 1.5 and the wall temperature.

The case of subsonic laminar flow at M=0.22 past a swept wing, at eight degrees angle of attack, is also computed. The inviscid flow solution is obtained by solving the potential flow equations numerically and then is interpolated at the desired boundary layer grid. Reference [14] presented informations about this method for the case of subsonic flow over ellipsoid. The solution at the leading edge attachment line and the solution of the local infinite swept wing at the root section are used as initial condition lines for the 3-D boundary layer calculations. Typtical results for the skin friction coefficients are shown in Figure 9.

Inconclusion, the present fourth-order accurate numerical method is capable to compute and predict the three-dimensional boundary layers over configurations with aeropsace interest, in both subsonic and supersonic flow - cases in an efficient and stable way.

REFERENCES

1. Smith, P. D., "The Numerical Computation of 3-D Boundary Layers," IUTAM Symposium, Berlin, Germany, Edited by H. Fernbolz and E. Krause, Springer Verlag, (1982).

2. Cousteix, J, "Three-Dimensional and Unsteady Boundary Layer Computations," Ann. Rev. Fluid Mech., Vol. 18, (1987).

3. Wang, K. C., "Boundary Layer over a Blunt Body at Low Incidence with Circumferential Reversed Flow," J. Fluid Mech., Vol. 72, Part I, (1975), pp. 49 .

4. Cebeci, T., Khattab, A. K., and Stewartson, K., "Three-Dimensional Laminar Boundary Layers and the OK of Accessibilty, " J. Fluid Mech., Vol. 107, (1981), pp. 57-87.

5. Radwan, S. F., "Numerical Solution of the Three-Dimensional Boundary Layer Equations in the Inverse Mode Using Finite-Differences," Ph. D. Thesis, Georgia Institute of Technology, U.S.A. (1985).

6. Radwan, S. F., and Lekoudis, S. G., "Boundary Layer Calculations in the Inverse Mode for Incompressible Flows Over Infinite Swept Wings," AIAA J., Vol. 22, No. 6, (1984).

7. Radwan, S. F., and Lekoudis, S. G., "Calculations of the Incompressible Turbulent Boundary Layers on an Ellipsoid in Inverse Mode," AIAA J., Vol. 24, NO. 10, (1986).

8. Wornom, S. F., "A Critical Study of High-Order Numerical Methods for Solving the Boundary Layer Equations," AIAA Paper No. 77-637, (1977).

9. Liniger, Werner, and Willoughby, R. A., "Efficient Integration Methods for Stiff Systems of Ordinary Differential Equations," SIAM J. Numer. Anal., Vol. 7, No. 1, March (1970), pp. 49.

10. Krause, E., Hirschel, E., and Boltman, "Numerical Stability of Three -- Dimensional Boundary Layer Solutions," Z. Angew Math. and Mech., Vol. 48, No. 8, (1968).

11. Keller, H. B., "Numerical Methods for Two-Point Boundary Value Problems," Blaisdell Pub. Co., (1968).

12. Cebeci, T., "Calculation of 3-D Boundary Layers, I. Swept Infinite Cylinders and Small Cross Flows," AIAA J., Vol. 12, (1974).

13. Fillo, J. A., and Burbank, R., "Calculation of 3-D Laminar Boundary Layer Flows," AIAA J., Vol. 10, (1972).

14. Radwan, S. F., "Higher Order Accurate Calculations of the Compressible Boundary Layers on A Prolate Spheroid," AIAA Paper No. 88-3586 , (1988).
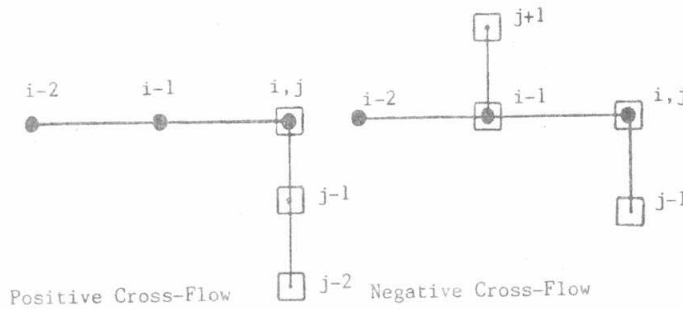
Figure 1. Finite-difference molecule of the present scheme
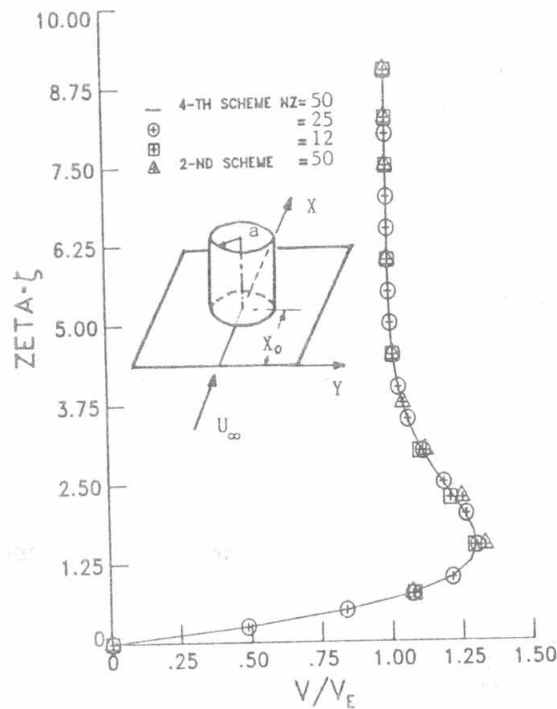
Figure 2. The computed crosswise velocity profiles at X=19.52 cm and Y=3.05 cm, for different total grid points NZ.
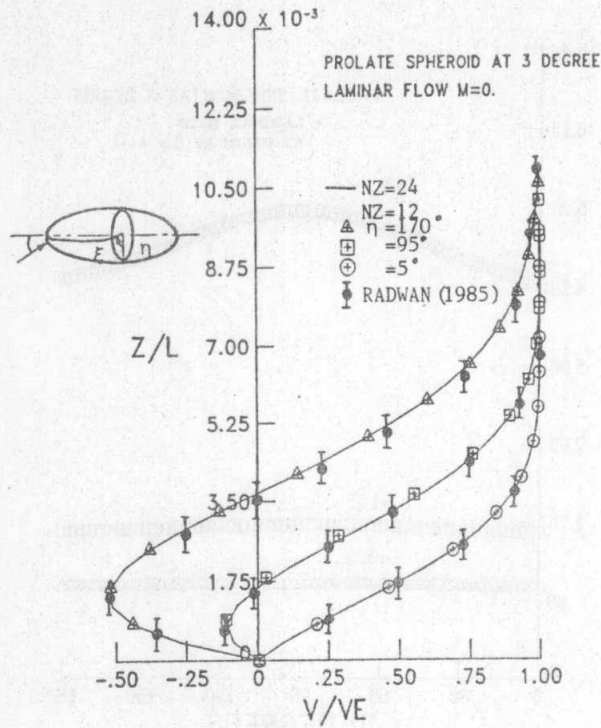
Figure 3. The cross-wise velocity profiles at
ξ =1.52 for flow over ellipsoid at
3° incidence.
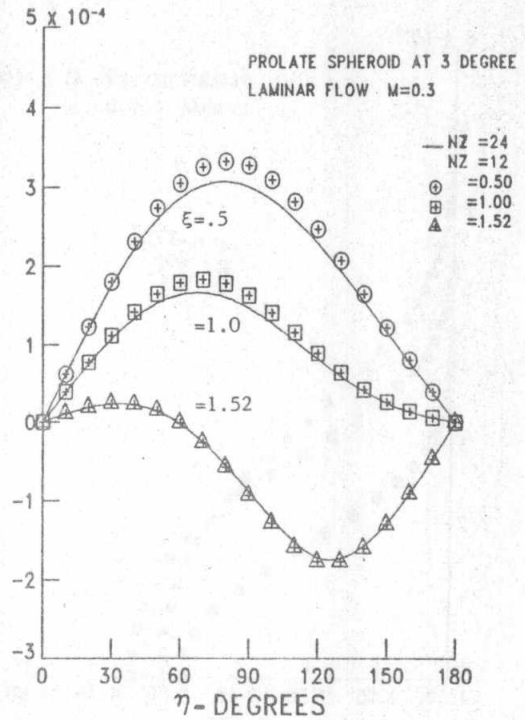
Figure 4. The cross-wise skin friction
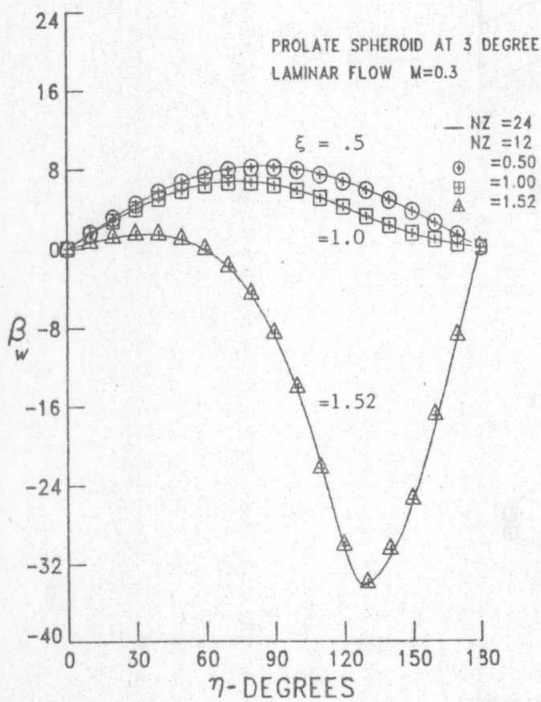coefficients for flow over
ellipsoid at 3° incidence.

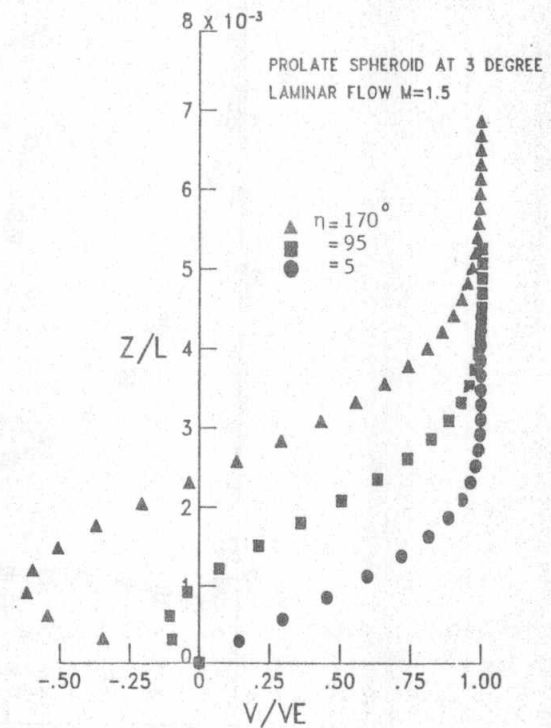Figure 5. The wall flow directions for flow
over ellipsoid at 3°incidence.

Figure 6. The computed cross-wise velocity
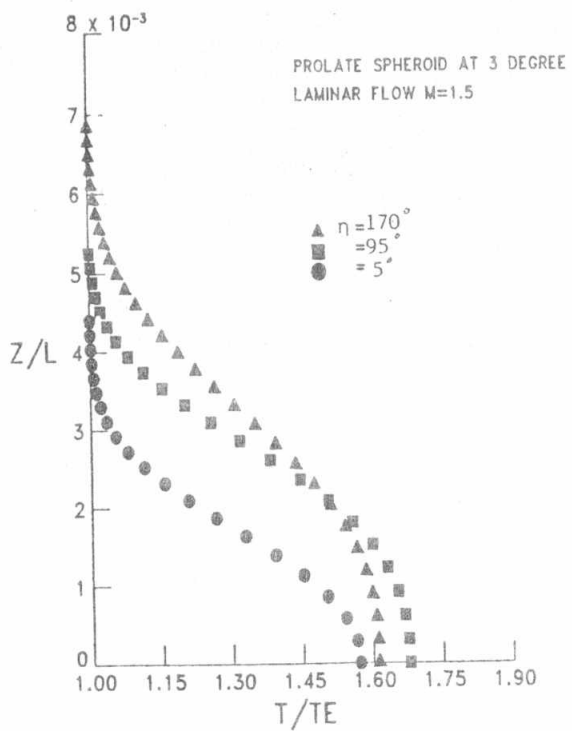profiles at ξ =1.5, for supersonic
flow over ellipsoid at 3°incidence.

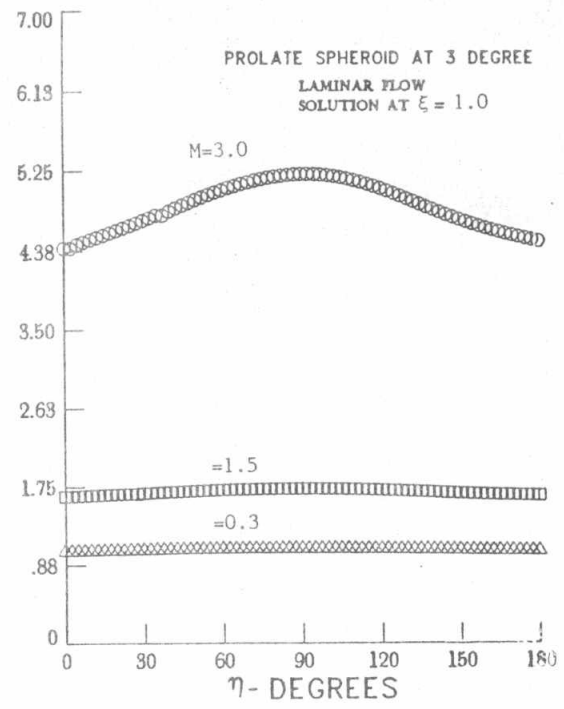Figure 7. The computed temperature profiles at $\xi=1.5$, for supersonic flow over ellipsoid at 3 incidence

Figure 8. The computed wall temperature profiles for different mach number flows over ellipsoid at 3 incidence
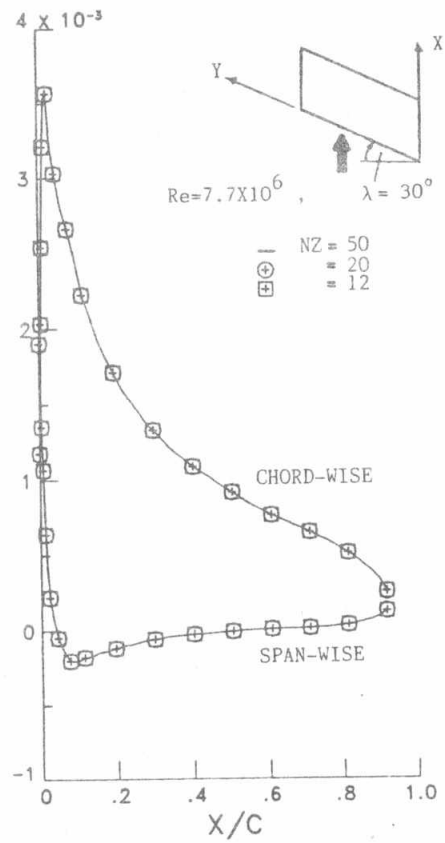

Figure 9. Computed skin friction coefficient near the root section of NACA-0012 swept wing at 8 incidence and M=0.22 .